

# Universal properties of a single polymer chain in slit: Scaling versus MD simulations

D.I.Dimitrov,

*Inorganic Chemistry and Physical Chemistry Department,  
University of Food Technology, Maritza Blvd.26,4002 Plovdiv,Bulgaria*

A.Milchev,

*Institute for Chemical Physics,  
Bulgain Academy of Sciences,  
1113 Sofia Bulgaria and Institut für Physik,  
Johannes Gutenberg-Universität Mainz  
D-55099 Mainz, Staudinger Weg 7, Germany*

Kurt Binder

*Institut für Physik, Johannes Gutenberg-Universität Mainz  
D-55099 Mainz, Staudinger Weg 7, Germany*

Leonid I. Klushin

*American University of Beirut, Department of Physics, Beirut, Lebanon*

Alexander M. Skvortsov

*Chemical-Pharmaceutical Academy, Prof. Popova 14, 197022 St. Petersburg, Russia.*

(Dated: October 26, 2018)

We revisit the classical problem of a polymer confined in a slit in both of its static and dynamic aspects. We confirm a number of well known scaling predictions and analyse their range of validity by means of comprehensive Molecular Dynamics simulations using a coarse-grained bead-spring model of a flexible polymer chain.

The normal and parallel components of the average end-to-end distance, mean radius of gyration and their distributions, the density profile, the force exerted on the slit walls, and the local bond orientation characteristics are obtained in slits of width  $D = 4 \div 10$  (in units of the bead radius) and for chain lengths  $N = 50 \div 300$ . We demonstrate that a wide range of static chain properties in normal direction can be described *quantitatively* by analytic model - independent expressions in perfect agreement with computer experiment. In particular, the observed profile of confinement-induced bond orientation, is shown to closely match theory predictions.

The anisotropy of confinement is found to be manifested most dramatically in the dynamic behavior of the polymer chain. We examine the relation between characteristic times for translational diffusion and lateral relaxation. It is demonstrated that the scaling predictions for lateral and normal relaxation times are in good agreement with our observations. A novel feature is the observed coupling of normal and lateral modes with two vastly different relaxation times.

We show that the impact of grafting on lateral relaxation is equivalent to doubling the chain length.

PACS numbers: 36.20-r, 36.20.Ey, 02.70.Lq

## I. INTRODUCTION

One of the most impressive successes in the theory of polymer solutions was the discovery of a close analogy with critical phenomena in ferromagnetic systems<sup>1,2,3,4,5</sup>: scaling theory based on this analogy predicts that in the case of a good solvent and flexible polymers the variation with molecular mass and concentration of many properties directly measured experimentally can be presented in universal form as functions of a dimensionless parameter - the ratio of a characteristic length to the average size of a polymer coil (Flory radius<sup>6</sup>)  $R_F = aN^\nu$  with the Flory index  $\nu \approx 3/5$  in dilute solution. Here  $a$  is the size of an effective monomeric unit and  $N$  - the number of such units in a polymer chain whereby, for simplicity, a prefactor of an order of unity is suppressed. For example, the mean-squared distance between monomers, mean-squared radius of gyration, static structure factors, were presented in scaling form<sup>4</sup>. The results were also generalized to include the effects of varying spatial dimensionality, solvent quality, and chain stiffness. Most of these predictions were verified both experimentally and by computer simulations. In fact, for an athermal isolated flexible macromolecule in three or two dimensions the level of description is so detailed that it includes not only the average characteristics but the probability distribution of the gyration radius,  $R$ , the two-point correlation functions and the average number of intramolecular contacts as a function of  $R$ .

The scaling theory was then extended to treat the effects of interfaces and geometrical restrictions. This direction of research is strongly motivated by important applications to colloid stabilization and flocculation, liquid chromatography, osmotic-pressure chromatography, ultrafiltration and others. A number of problems are thereby closely related to the adsorption of polymers at surfaces and interfaces. However, even in the absence of adsorption, geometric constraints imposed on a polymer induce dramatic changes in its behavior which have consequences pertaining to important applications. The basic model that captures almost all the essential physics is a single polymer chain in a slit or a tube with neutral (repulsive) walls<sup>7,8,9,10,11,12,13,14,15,16,17,18,19,20,21,22,23,24,25,26,27,28,29</sup>. Lately, the main focus has shifted to semidilute and concentrated solutions<sup>25,30,31</sup>. Nevertheless, even the basic model has intriguing properties some of which have not been fully clarified yet.

The presence of a solid impenetrable wall gives rise to depletion effects that were successfully treated within the scaling framework<sup>32,33,34,35</sup> and found experimental verification. The most dramatic effects are observed when long polymer chains are confined in slit-like or tube-like nanochannels where the chains become effectively two- or one-dimensional. This situation is typical for biological objects in living matter. Scaling theory formulated by de Gennes<sup>2,7,8</sup> describes the basic polymer characteristics, namely the average size of a chain and its confinement free energy. It is well understood that the scaling expressions are valid only asymptotically:  $R \gg D \gg a$ , otherwise corrections to scaling come into play. The scaling predictions have been successfully tested<sup>27,28</sup> by means of Monte-Carlo simulation methods<sup>36</sup>.

In this paper we present the results of detailed Molecular Dynamics (MD) simulations using a coarse-grained bead-spring model with the aim of establishing the range of validity of the scaling theory for uncharged flexible polymers in good solvent strongly confined in a slit. One of the goals of the paper is to give simple expressions that provide numerically accurate values for all the essential characteristics of the chain with regard to the polymerization index,  $N$ , and the slit width  $D$ .

We analyse the principle conformational parameters (end-to-end distance  $r$  and the gyration radius  $R$ ) for both lateral and normal directions. We examine the probability distributions  $W(r)$  and  $W(R)$  for the lateral components of  $r$  and  $R$ , establish their universal character and provide simple analytical expressions for them. Special attention is paid to the properties in *normal* direction which have been largely ignored in earlier studies. Thus we derive analytic expressions for the normal components of  $\langle r^2 \rangle$  and  $\langle R^2 \rangle$  which turn to be model-independent, in perfect agreement with the simulation data. The bond orientation profile across the slit as well as the mean bond orientation against slit width  $D$  have been predicted analytically and verified here by computer experiment. The average force produced by the polymer on the confining walls is calculated directly, suggesting thus a scaling form for the free energy of confinement with accurate numeric coefficients.

An essential part of our investigation examines dynamical properties of polymers in confinement. We calculate the time autocorrelation functions for the gyration radius and the end-to-end distance, extract the relaxation times, and demonstrate distinct dynamic scaling behavior for lateral and normal relaxation as well as their mutual interplay.

Recently discovered possibilities of manipulating individual chains by AFM, optical tweezers and surface force apparatus have generated strong interest in the properties of end-grafted chains subject to external forces and confinement effects<sup>38,39</sup>. In view of these developments we present a theoretical analysis and MD simulation data on the effects of grafting with respect to the static and dynamic characteristics of the polymer.

The paper is organized as follows: In Section II we give a brief description of the model, and in Section III we discuss the properties of a confined chain in equilibrium. We give a derivation of the bond orientation profile across the slit in the Appendix. Section IV examines the relaxational and diffusive dynamics of the polymer. Finally we discuss the implications of our results in Section V.

## II. MODEL AND METHOD

The setup of our simulation is displayed in Figure 1. The polymer chains are described by a simple coarse-grained bead-spring model, originally proposed by Kremer and Grest<sup>37</sup>, which has been widely and very successfully used for MD simulations of polymers in various contexts<sup>40,41</sup>. Effective monomers along the chain are bound together with a finitely-extensible non-linear elastic (FENE) potential,

$$U_{FENE}(\mathbf{r}) = -15\epsilon_w(\mathcal{R}_0/\sigma)^2 \ln(1 - \mathbf{r}^2/\mathcal{R}_0^2), \quad \mathcal{R}_0 = 1.5\sigma \quad (1)$$

where  $\sigma$  is the range parameter of a purely repulsive Lennard-Jones (LJ) potential, that is truncated and shifted to zero in its minimum and acts between any pairs of monomers.

$$U_{LJ}(\mathbf{r}) = 4\epsilon [(\sigma/\mathbf{r})^{12} - (\sigma/\mathbf{r})^6 + 1], \quad \mathbf{r} \leq \mathbf{r}_c = 2^{1/6}\sigma \quad (2)$$

The parameter  $\epsilon$ , characterizing the strength of this potential, is chosen unity, also the temperature  $k_B T \equiv 1$ , thus this potential gives rise to an excluded volume interaction between all the non-bonded monomers of the chain; for

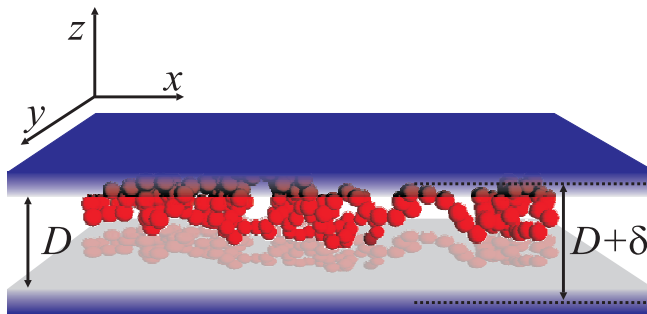


FIG. 1: A snapshot of a tethered chain with  $N = 200$  monomers in a slit of width  $D = 4.0$ . The soft repulsion of the wall potential is indicated by a gradient in the color intensity. The *effective* width  $D + \delta$  is indicated by dashed lines. The grafting monomer is indicated by darker color.

the bonded monomers, together with  $U_{FENE}(\mathbf{r})$ , it leads to a typical neighbor - neighbor distance of  $\mathbf{r}_{min} = 0.96\sigma$ . Henceforth we choose  $\sigma = 1$  as our unit of length.

Similarly, the confining walls are presented also by a purely repulsive wall defined by Eq. 2 whereby the wall position is placed at the potential minimum.

Molecular Dynamics (MD) simulations were performed using the standard Velocity-Verlet algorithm<sup>42</sup>, carrying out typically  $1.5 \times 10^9$  time steps with an integration time step  $\delta t = 0.01t_0$  where the MD time unit (t. u.)  $t_0 = (\sigma^2 m / 48 \epsilon_{LJ})^{1/2} = 1/\sqrt{48}$ , choosing the monomer mass  $m = 1$ . The temperature was held constant by means of a standard Langevin thermostat with a friction constant  $\zeta_0 = 0.5$

### III. GLOBAL EQUILIBRIUM CHARACTERISTICS

#### A. Free Energy and Force

According to the blob picture<sup>2</sup>, a chain confined in a narrow slit of width  $D$  will form a two-dimensional self-avoiding walk consisting of  $n_b$  blobs of size  $D$ . Each blob contains  $g = (D/a)^{1/\nu}$  monomers so that the number of blobs is  $n_b = N/g = N(D/a)^{-1/\nu}$  where  $a$  is the distance between neighboring monomers, and  $\nu = 0.58758(7)$ <sup>27</sup> is the Flory index in 3-dimensional space. The free energy excess of the confined chain (in units of  $k_B T$ ) is simply the number  $n_b$  of blobs,

$$F_{\text{conf}} = B n_b = B N (D/a)^{-1/\nu}, \quad (3)$$

where  $B$  is a model-dependent dimensionless numerical coefficient. Note that this free energy is extensive in  $N$ .

The confinement free energy and the associated force acting on the walls were studied<sup>27,29</sup> by means of the pruned-enriched Rosenbluth method (PERM algorithm) that allows one to estimate the partition function<sup>36</sup>. For the off-lattice model of Ref.<sup>17</sup>, the pressure tensor was calculated using the virial theorem and studied in conjunction with the normal density profile. For relatively narrow slits the simulation data for the force were consistent with the scaling prediction  $f \approx N D^{-1-1/\nu}$ .

For self-avoiding walks on a simple cubic lattice the confinement free energy was calculated by MC methods in<sup>26,27</sup>. These results were presented by a general power-law fit as  $F_{\text{conf}} = 0.843 N^{0.94} (D/a)^{-1.57}$ . According to this fit, the free energy is not exactly extensive and the  $D$ -exponent deviates from the scaling prediction which makes the fitting formula purely phenomenological. Hsu and Grassberger<sup>27</sup> have obtained accurate data for very long chains ( $N$  up to 8000 and slit width up to  $D = 120$ ) and verified the scaling prediction. They also noted that there must be a non-universal correction to the value of the slit width  $D$  to  $D + \delta$  with  $\delta = 0.33$ , since the original scaling formula assumes the asymptotic limit  $D \gg a$ . Their best fit for the confinement free energy was  $F_{\text{conf}} = 2.10 N (D/a)^{-1/\nu}$ . The importance of proper corrections to the slit width in order to achieve good scaling was emphasized by Milchev and Binder<sup>17</sup> and by Teraoka<sup>28</sup>.

The MD method does not allow to obtain the free energy, but the force acting on the walls can be calculated directly. The force acting on the walls is directly derived from the confinement free energy

$$f a = -dF_{\text{conf}}/dD = (B/\nu) N (D/a)^{-1-1/\nu} \quad (4)$$

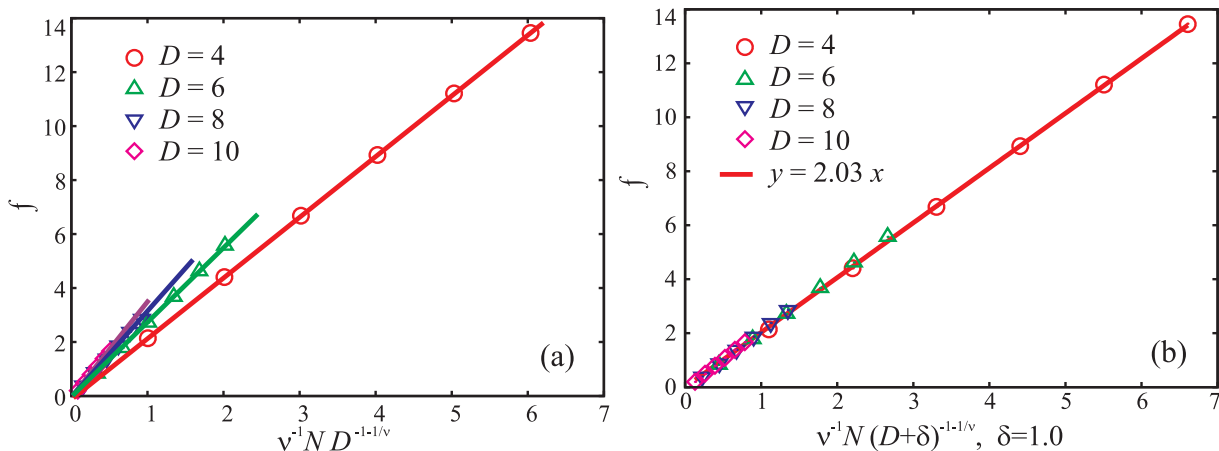


FIG. 2: Variation of the force  $f$ , exerted by a confined polymer chain on the slit walls, with scaling variable  $\nu^{-1}ND^{-1-1/\nu}$ : (a) without, and (b) with taking the width correction  $\delta$  into account.

Figure 2 presents the force against the scaling combination  $N(D/a)^{-1-1/\nu}$  with and without a shift  $\delta$ . It is clear from Figure 2 that the data points do not fall on a universal curve, if  $\delta = 0$ . The best universal fit for the force was obtained for  $\delta = a$ :

$$fa = 2.03\nu^{-1}ND^{-1-1/\nu}. \quad (5)$$

The corresponding free energy is given by

$$F_{\text{conf}} = 2.03N(D/a + 1)^{-1/\nu} \quad (6)$$

This correction to  $D$  turned out to be relevant not only for the free energy but for describing the variation of all other quantities as functions of  $D$  too. Throughout the paper we use the same slit width correction  $\delta = a$ . It is remarkable that the scaling asymptotic relation for the confinement free energy is achieved very early, when the number of blobs is still close to unity: the minimal number of blobs in our simulations was  $n_b = N(D/a + 1)^{-1/\nu} = 0.84$  for  $N = 50$  and  $D = 10$ .

Comparing our results for the free energy with those obtained for a lattice model we notice that a very good semi-quantitative estimate of the slit confinement free energy is  $2k_B T$  per blob. It is also quite remarkable that the same estimate<sup>29</sup> works very well for the free energy of a  $2D$  chain confined in a strip ( $F_{\text{conf}} = 1.944n_b$  where  $n_b = ND^{-1/\nu_2}$ ).

## B. Density profiles

The distribution of the end monomer position across the slit was studied extensively by Hsu and Grassberger<sup>27</sup>. The scaling variable is taken as the ratio  $\xi = z/D$  and a simple scaling formula that takes into account the mirror symmetry with respect to the median plane was proposed. If the coordinate  $z$  is counted from the median plane, the expression has the following form

$$\rho_{\text{end}}(\xi) = \frac{\Gamma(2 + 1/\nu)}{\Gamma^2(1 + 1/2\nu)} (1/4 - \xi^2)^{1/2\nu} \quad (7)$$

The distribution Eq. 7 is properly normalized to unity. It is well known that for an ideal chain in a slit the total monomer density profile is proportional to the square of the end segment distribution, as long as the strong confinement condition is satisfied. A hypothesis that the same relation holds also for self-avoiding chains was checked by Hsu and Grassberger<sup>27</sup> and good agreement was observed. With this ansatz, the monomer density profile can be written as

$$\rho(\xi) = \frac{\Gamma(2 + 2/\nu)}{\Gamma^2(1 + 1/\nu)} (1/4 - \xi^2)^{1/\nu} \quad (8)$$

Density distributions of end-monomers and of all monomers across the slit width (for tethered chains of different length  $N$  and slits of different width  $D$ ) are presented in Figure 3 together with the theoretical curves. The data

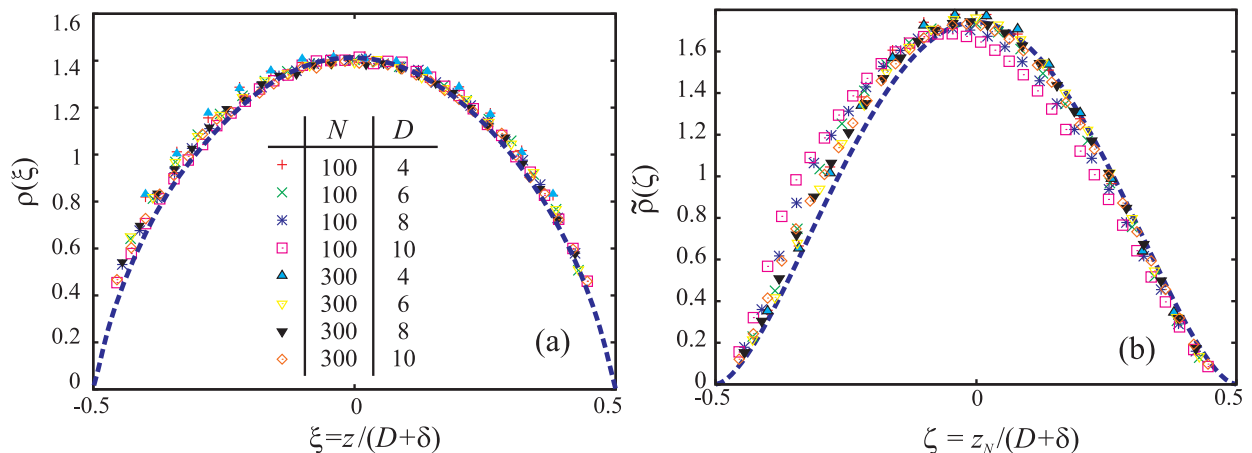


FIG. 3: Density distribution of end-monomers (a), and all monomers (b), across the slit width for tethered chains of different length  $N$  and slits of different width  $D$  (both given as parameters). Dashed lines denote the theoretical results, see Eqs. 7, 8.

points for various values of  $N$  and  $D$  collapse onto the universal theoretical curves containing no fitting parameters. Some deviations violating the mirror symmetry can be seen on the full density distribution picture. These are due to the effects of grafting which are especially noticeable for the shortest chain  $N = 100$  in a wide slit  $D = 10a$ . The fact that the analytical formulae based on the scaling ansatz work very well both for the end monomer distribution and the full density profile for lattice as well as for off-lattice models is quite remarkable.

The scaling ansatz has been also verified by Hsu and Grassberger<sup>29</sup> for two-dimensional chains (with  $\nu_2 = 3/4$ ) confined in a strip, and for confined ideal chains (with  $\nu_G = 1/2$ ) in a slit. We would confidently speculate that the formulae will work for real flexible polymers in good and  $\theta$ -solvents including exotic situations when strong adsorption enforces essentially 2D conformations while additional repulsive barriers confine the chain inside a strip.

### C. Average chain size characteristics.

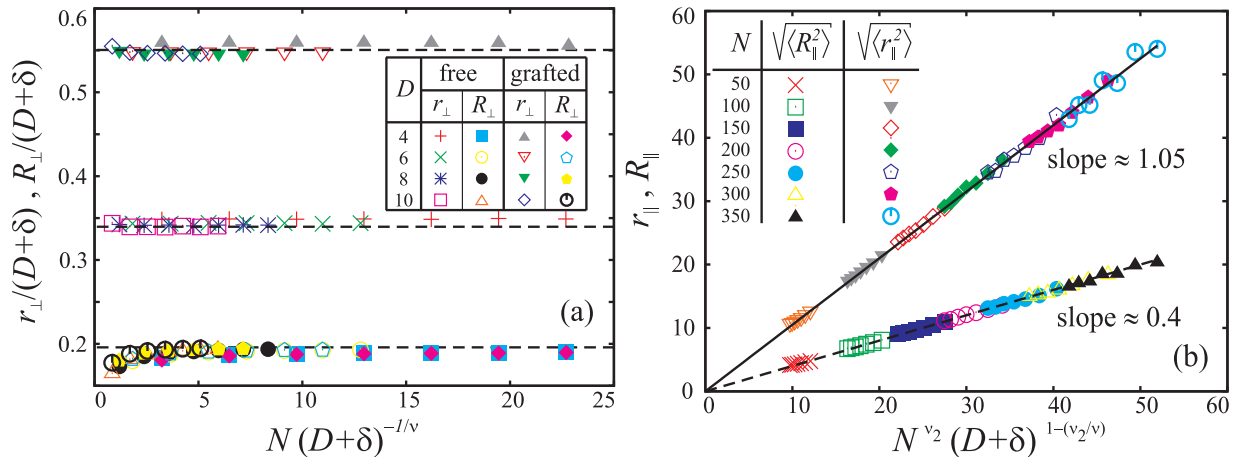


FIG. 4: (a) Normal components of the end-to-end vector,  $r_{\perp}$ , and the gyration radius,  $R_{\perp}$ , against the number of blobs  $N(D + \delta)^{-1/\nu}$ . (b) Variation of the parallel components of the end-to-end vector,  $r_{\parallel}$ , and gyration radius,  $R_{\parallel}$ , with scaling variable  $N^{\nu_2} (D + \delta)^{1-\nu_2/\nu}$  for chains of length  $N$  and different slit width  $4 \leq D \leq 10$ .

The characteristics for a polymer chain average size can be reduced to moments of the joint monomer-monomer

distribution  $\hat{\rho}(z_i, z_j)$ . In particular, the mean square of the gyration radius  $\langle R_{\perp}^2 \rangle$  is calculated as:

$$\langle R_{\perp}^2 \rangle = (1/2N) \sum_{i,j=1}^N \int \int (z_i - z_j)^2 \hat{\rho}(z_i, z_j) dz_i dz_j \quad (9)$$

whereby the integration in Eq. 9 is carried out across the slit. It follows naturally from the scaling blob picture of a chain strongly confined in a slit that the joint distribution splits into a product of single-monomer distributions  $\hat{\rho}(z_i, z_j) = \rho(z_j)\rho(z_i)$  as long as the monomers are separated along the chain by at least one blob,  $|j - i| D^{1/\nu}$ . We assume that the dominant contribution comes from the internal monomer pairs (that is, pairs which do not belong to the two terminal blobs). Hence the single-monomer distribution  $\rho(z_j)$  is independent of the index  $j$  and coincides with the normalized full density profile  $\rho(z)$ . It follows that

$$\begin{aligned} \langle R_{\perp}^2 \rangle &= \frac{1}{2} \int \int (z - z')^2 \rho(z) \rho(z') dz dz' \\ &= \left[ \frac{1}{4} + \frac{\Gamma(2 + \frac{2}{\nu})}{\Gamma(1 + \frac{1}{\nu})} \left( \frac{\Gamma(3 + \frac{1}{\nu})}{\Gamma(4 + \frac{2}{\nu})} - \frac{\Gamma(2 + \frac{1}{\nu})}{\Gamma(3 + \frac{2}{\nu})} \right) \right] D^2 \end{aligned} \quad (10)$$

i. e.,  $\langle R_{\perp}^2 \rangle = 0.04D^2$ , where the scaling form of the full density was used. The derivation suggests that effects of grafting should not be discernable in  $\langle R_{\perp} \rangle$ . The average square of the normal end-to-end distance is defined as

$$\langle r_{\perp}^2 \rangle = \int \int (z_1 - z_N)^2 \hat{\rho}(z_1, z_N) dz_1 dz_N \quad (11)$$

We employ the same factorization assumption to separate the probability densities for the two chain ends. In the case of a non-grafted chain both ends are described by  $\rho_{\text{end}}(z)$  distributions leading to

$$\begin{aligned} \langle r_{\perp}^2 \rangle &= \int \int (z_1 - z_N)^2 \rho_{\text{end}}(z_1) \rho_{\text{end}}(z_N) dz_1 dz_N \\ &= \left[ \frac{1}{2} + \frac{2\Gamma(2 + \frac{1}{\nu})}{\Gamma(1 + \frac{1}{2\nu})} \left( \frac{\Gamma(3 + \frac{1}{2\nu})}{\Gamma(4 + \frac{1}{\nu})} - \frac{\Gamma(2 + \frac{1}{2\nu})}{\Gamma(3 + \frac{1}{\nu})} \right) \right] D^2 \\ &= 0.1D^2. \end{aligned} \quad (12)$$

If one end is fixed (tethered) at some point  $z_{gr}$ , then the distribution for this end is given by  $\rho(z_1) = \delta(z_1 - z_{gr})$  reducing the formula to  $\langle r_{\perp}^2(z_{gr}) \rangle = \langle r_{\perp}^2(0) \rangle + z_{gr}^2$  where

$$\langle r_{\perp}(0)^2 \rangle = \left( \frac{\Gamma(3 + \frac{1}{2\nu})\Gamma(2 + \frac{1}{\nu})}{\Gamma(4 + \frac{1}{\nu})\Gamma(1 + \frac{1}{\nu})} - \frac{1}{4} \right) D^2 \quad (13)$$

The result is quite general and covers a whole class of confined systems characterized by different values of the Flory index  $\nu$ . In our model the chain end was fixed at  $z_{gr} = D/2 - 1$  and the simulation data are to be compared to the theoretical expression

$$\langle r_{\perp}^2 \rangle_{gr} = 0.3D^2 - D + 1 \quad (14)$$

The formula suggests that the combination

$$D^{-1} \sqrt{\langle r_{\perp}^2 \rangle_{gr} + D - 1} \quad (15)$$

remains constant independent of  $D$  and  $N$ . Strictly speaking, the above theoretical predictions are valid only asymptotically for  $n_b \gg 1$ . The simulation data for the three characteristics calculated above are presented in Figure 4a as functions of the blob number. The end-to-end distance for the grafted chains is corrected according to Eq. 15. In full agreement with the asymptotic theory, the normalized values are independent of  $D$  and  $N$ , and the actual values coincide with the theoretical predictions. Small deviations are visible only for the gyration radius curve with number of blobs close to 1. It is quite remarkable that the limiting asymptotic values are achieved even for such moderate compression.

It is well known that the size of a free chain in the bulk is proportional to  $N^\nu$ . For the Kremer-Grest model<sup>37</sup> that we use in our MD simulations, the model-dependent numerical prefactors defining the rms average of the gyration radius and the end-to-end distance have been estimated as

$$R_F = 0.27aN^\nu \text{ and } r_F = 0.67aN^\nu. \quad (16)$$

According to the blob picture, a chain in a slit is a two-dimensional self-avoiding walk consisting of  $n_b$  blobs of size  $D$ . Thus scaling predicts the average lateral size to be

$$R_{\parallel} \sim n_b^{\nu_2} D = aN^{\nu_2} (D/a)^{1-\nu_2/\nu}. \quad (17)$$

If  $D$  is of the same order as  $R_F$ , Eq. (17), one finds  $R_{\parallel} \sim aN^\nu$ , providing the expected smooth crossover.

Figure 4b presents the average lateral  $r_{\parallel}$  component of the end-to-end distance and the gyration radius versus the scaling arguments as suggested by the theory. For the lateral size, no effect of grafting was observed.

The best fit for the average lateral end-to-end distance is

$$r_{\parallel} = 1.05aN^{\nu_2} (D/a + 1)^{1-\nu_2/\nu} \quad (18)$$

and for the average lateral component of the gyration radius

$$R_{\parallel} = 0.40aN^{\nu_2} (D/a + 1)^{1-\nu_2/\nu} \quad (19)$$

Although the amplitudes are non-universal, it would have been instructive to compare them to those of other models in order to see the variation range. Unfortunately, only one amplitude for the end-to-end distance of chains on a cubic lattice  $r_{\parallel} = 0.835aN^{\nu_2} (D/a + 1)^{1-\nu_2/\nu}$  could be found in the literature<sup>29</sup>.

#### D. Probability distributions of end-to-end distance and radius of gyration

The scaling form for the end-to-end vector distribution of a self-avoiding polymer chain was suggested by Fisher<sup>43</sup> in 1966 and then refined by Cloizaux<sup>4</sup> and others. In the MD simulations we obtain the histogram for the scalar end-to-end distance. The distribution for the reduced scalar distance  $\eta = (r/r_0)$  in  $d$  dimensions can be represented as

$$W_d(\eta) = Ar_0^{-1}\eta^{(d-1)}\eta^{\theta_d} \exp(-B\eta^{\delta_d}) \quad (20)$$

where  $r_0$  is the average end-to-end distance, and  $A$  and  $B$  are numerical coefficients. The exponent  $\delta_d = 1/(1 - \nu_d)$  describes strong stretching of the chain and is related to the Flory exponent  $\nu_d$  for a chain in the  $d$ -dimensional space. The exponent  $\theta_d = (\gamma_d - 1)/\nu_d$  is related to another critical exponent  $\gamma_d$  that appears in the partition function  $Q_N = \mu^{-N} N^{\gamma_d - 1}$  where  $\mu$  is called an *effective* coordination number. In  $d = 2$  one has  $\gamma_2 = 43/32^1$ , in  $d = 3$  the best estimate is  $\gamma_3 = 1.1575(6)^{44}$ . The extra factor  $r_0^{-1}\eta^{(d-1)}$  that appears in Eq. 20 in comparison to the cited references is due to the volume element included in the definition of the distribution of the scalar distance. According to this definition, the two normalization conditions have the following form:  $\int W_d(r)dr = 1$  and  $\int rW_d(r)dr = r_0$ , and they fix uniquely the values of  $A$  and  $B$ :

$$B = \left[ \Gamma\left(\frac{d+1+\theta_d}{\delta_d}\right) / \Gamma\left[\frac{d+\theta_d}{\delta_d}\right] \right]^{\delta_d} \quad (21)$$

$$\begin{aligned} A &= \frac{\delta_d}{\Gamma\left(\frac{d+\theta_d}{\delta_d}\right)} \left[ \Gamma\left(\frac{d+1+\theta_d}{\delta_d}\right) / \Gamma\left[\frac{d+\theta_d}{\delta_d}\right] \right]^{(d+\theta_d)} \\ &= 1.374 \end{aligned} \quad (22)$$

The final form of  $W_d(\eta)$  for  $d = 2$  is

$$W_2(\eta) = 1.374\eta^{1.458} \exp(-0.324\eta^4) \quad (23)$$

For  $d = 3$  the distribution is given by

$$W_3(\eta) = 3.032\eta^{2.268}\exp(-1.084\eta^{2.425}) \quad (24)$$

It is clear that the distribution  $W(\eta)$  for a finite chain in a slit has to be between  $W_2$  and  $W_3$ . For narrow slits and long chains,  $r_0 \gg D$ , the distribution  $W(r)$  is expected to be close to  $W_2$ . For wide slits or short chains with  $r_0 \approx D$ ,  $W(\eta)$  should be closer to the three-dimensional distribution  $W_3$ .

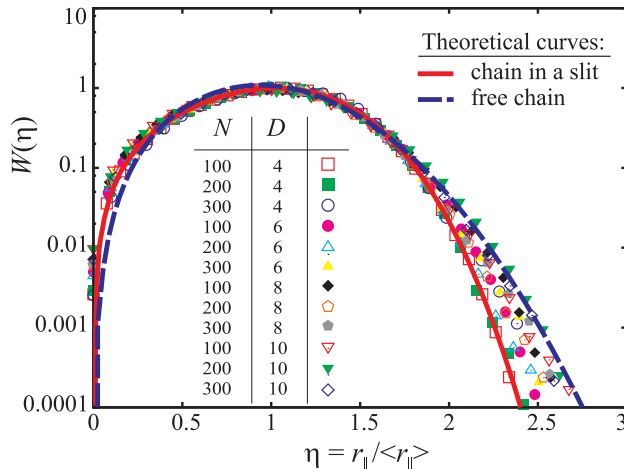


FIG. 5: Probability distribution functions of the end-to-end distance of a polymer chain parallel to the slit wall for varying chain length  $N$  and slit width  $D$ . Lines indicate the analytic results for a confined chain (full line), Eq. 23, and for a chain without geometric constraints, Eq. 24, (dashed line). The curves are normalized so that the average value  $\langle \eta \rangle = 1$  and  $W(\langle \eta \rangle) = 1$ .

In Figure 5 we plot the distribution  $W(\eta)$  of the lateral component of the end-to-end distance (in semi-log scale) against  $\eta = r/r_0$  for various chain lengths  $N$  and slit widths  $D$ . The analytical equations  $W_2$  and  $W_3$  for chains in two-dimensions and three-dimensions are shown by solid and dotted lines, respectively. In the region around the maximum both distributions are close to each other and all data points collapse on a universal curve. For large extensions  $r > 1.8r_0$ , the strongly confined chains follow the two-dimensional curve  $W_2$  while for chains in relatively wide slits the data points lie closer to the three-dimensional curve  $W_3$ . In this region  $W(\eta)$  is not universal and depends on the ratio  $r_0/D$ . The distribution of the gyration radius for a chain in a narrow tube was postulated by Victor<sup>23</sup> in scaling form, and verified numerically by Sotta et al.<sup>21</sup> and Bishop et al.<sup>22</sup>. They also calculated the probability distribution for the end-to-end distance and fitted their results by a similar expression. The distribution of the gyration radius and of the end-to-end distance for a chain in a slit has not been analyzed yet.

In Figure 6 we plot the distribution  $R_{\parallel}$  of the lateral component of the gyration radius (in semi-log scale) vs  $\zeta = R_{\parallel}/R_0$  for various chain lengths  $N$  and slit widths  $D$ . The analytical equations  $W_2$  and  $W_3$

$$W_2(\zeta) = 0.65 (\zeta^{-4} + \zeta^4 - 2) \quad (25)$$

and

$$W_3(\zeta) = 1.34 (\zeta^{-4} + \zeta^4 - 2) \quad (26)$$

for two-dimensional and three-dimensional chains are shown by solid and dotted lines, respectively. In the region around the maximum both distributions are close to each other and all data points collapse on a universal curve. For large extensions  $R > 1.8R_0$ , the strongly confined chains follow the two-dimensional curve  $W_2(\zeta)$  while for chains in relatively wide slits the data points lie closer to the three-dimensional curve  $W_3(\zeta)$ . In this region  $W(\zeta)$  is not universal and depends on the ratio  $R_0/D$ .

### E. Confinement effect on segment orientation

A commonly used measure characterizing the orientation of bonds is the average value of the second Legendre polynomial of the azimuthal angle,  $\langle P_2 \rangle = 2^{-1}(3(\cos^2 \theta) - 1)$ . Experimentally this parameter appears in NMR and



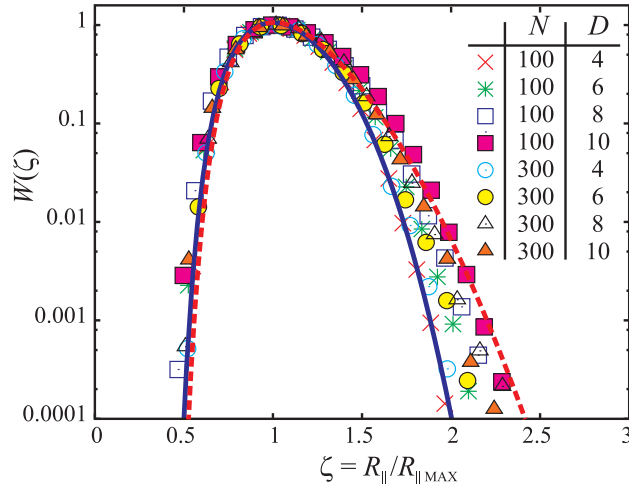


FIG. 6: Probability distribution functions of the gyration radius  $R_{\parallel}$ , parallel to the slit wall. Here curves are normalized so that the maximum value  $\zeta_{MAX} = 1$  and  $W(\zeta_{MAX}) = 1$ .

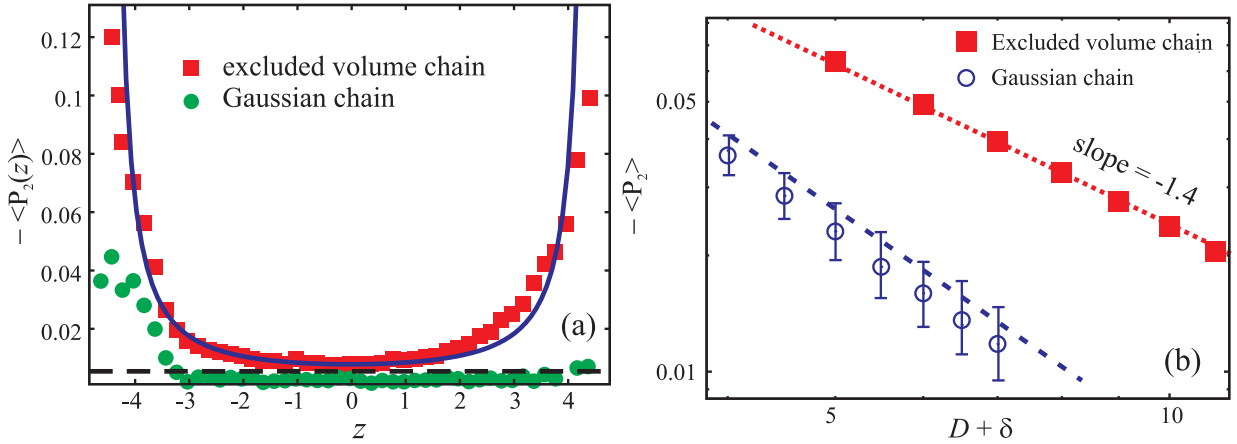


FIG. 7: (a) Profile of mean bond orientation  $\langle P_2(z) \rangle = 2^{-1} [3\langle \cos^2 \theta \rangle - 1]$  across the slit where the orientation of the bonds is measured with respect to the  $Z$ -axis, for a real and Gaussian tethered chain. A horizontal dashed line denotes the theoretical prediction,  $\langle P_2(z) \rangle_{\text{id}} = -\frac{\pi^2}{15}(a/D)^2$ , while a full line marks the scaling conjecture  $\langle P_2(z) \rangle \propto (D^2 - z^2)^{2(1-1/\nu)}$ . (b) Variation of  $\langle P_2 \rangle$ , averaged over  $z$ , against the effective slit width  $D + \delta$ . Circles denote simulation results for a Gaussian chain, squares - for a chain with excluded volume interactions. A dotted straight line indicates the theoretically predicted slope of  $-1.4$ , and a dashed line shows the theoretical result for  $\langle P_2 \rangle_{\text{id}}$ , Eq. 43.

optical birefringence measurements. In a free non-confined coil the bond orientation is completely isotropic, and  $\langle P_2 \rangle = 0$ . For a chain in a slit, it is natural to expect a preferential bond orientation along the lateral plane which would lead to a non-zero negative value of  $\langle P_2 \rangle$ . In Figure 7a the profile of the average orientation across the slit obtained in the MD simulation is displayed together with the similar profile calculated for the same model but with the excluded volume interactions between non-neighboring monomers switched off. The values of  $\langle P_2 \rangle$  averaged over all monomers irrespective of their position are plotted against the effective slit width in Figure 7b in a log-log scale, the best fit for the slopes being  $-2.0$  for the ideal chain, and  $-1.44$  for the 'real' chain (with excluded volume). It is clear that the excluded volume interactions affect the magnitude of the orientation very strongly.

A naive estimate of the orientation effect as a function of the slit width can be obtained as follows: assume that the wall induces some lateral orientation only locally, within a distance of the order of a monomer size  $a$ . The local orientation is by itself independent of  $D$ . The fraction of monomers within distance  $a$  from the wall is given by  $\rho(D/2 + a) \sim D^{-1-1/\nu}$  which would give  $D^{-2.70}$  for a chain with excluded volume and  $D^{-3}$  for an ideal chain. Both estimates turn out to be well below the magnitude of the observed effect. Next, we introduce the effect of *orientation correlations* along the backbone of the chain. It is known that the simplest bond-bond orientation correlation function  $P_1$  for an ideal chain decreases exponentially with the distance  $s$  along the chain,  $\exp(-\kappa s)$  where  $\kappa \propto 1/a$  for flexible

chains. In a real chain the correlations decay according to a power law  $s^{-\omega}$  where  $\omega = 2(1 - \nu)^{45}$ . We will assume that the correlations that transmit the orienting effect of the wall, as described by the  $\langle P_2 \rangle$  parameter, propagate along the chain according to the same laws. In the spirit of the scaling theory, the contour distance  $s$  can be related to the normal distance from the wall,  $z$ , as  $s = z^{1/\nu}$ . Thus the relationship  $\langle P_2(z) \rangle \propto z^{-\omega/\nu}$  can be represented in a normalized form as  $\langle P_2(z) \rangle \propto (\frac{D^2}{4} - z^2)^{-2/\nu}$ . Figure 7a demonstrates that the simulation data appear in very good agreement with this theoretical prediction.

By integrating over the slit width one obtains the average orientation parameter for the real chain as

$$\langle P_2 \rangle = \langle P_2 \rangle_{wall} \int_{-D/2}^0 z^{-\omega/\nu} \rho(z) dz = const. D^{-\omega/\nu} \quad (27)$$

A similar calculation for the ideal chain gives

$$\langle P_2 \rangle = \langle P_2 \rangle_{wall} \int_{-D/2}^0 e^{-\kappa z} \rho_{id}(z) dz = const. D^{-3}. \quad (28)$$

It is clear that the scaling law obtained for the real chain,  $\langle P_2 \rangle \sim D^{-2(1/\nu-1)} = D^{-1.40}$  agrees very well with the simulation data while the theoretical result for the ideal chain  $\langle P_2 \rangle \sim D^{-3}$  still underestimates the observed effect. This suggests that apart from the local orienting effect of the wall there must be another mechanism inducing preferential orientation in the lateral plane. A theory describing this mechanism is given in the Appendix. The main result for the ideal chain is

$$\langle P_2 \rangle_{id} = -\frac{\pi^2}{15D^2} \quad (29)$$

which agrees well with the simulation data without any fitting parameters.

#### IV. DYNAMIC SCALING

There are only few simulation studies on the dynamics of a polymer chain confined in a slit. For such a chain only the center-of-mass diffusion has been studied by MC for an off-lattice model<sup>46</sup>. The characteristic diffusion time was found to scale as  $\tau \sim N^{5/2}$  which conforms to the dynamic scaling prediction  $\tau \propto R^2/N$  using the static scaling prediction  $R \sim N^{\nu_2}$ . Here we present a study of relaxation dynamics for the gyration radius, derived from the analysis of the appropriate autocorrelation functions, and compare it to the center-of-mass diffusion characteristic time. The time-dependent autocorrelation functions were calculated as follows:

$$\langle C_R(t) \rangle = \frac{\langle R(0)^2 R(t)^2 \rangle - \langle R(0) \rangle^2}{\langle R(0)^4 \rangle - \langle R(0) \rangle^2} \quad (30)$$

separately for the lateral and perpendicular components of the gyration radius.

Typical curves are presented in Figure 8. Part (a) demonstrates the effect of grafting one chain end. Evidently, this slows down considerably the lateral relaxation. The grafting effect on the normal relaxation is more complicated, and this is directly related to the shape of the ACF. The major initial portion of normal ACF is characterized by a rapid decay with a relaxation time *unaffected* by grafting. However, there is clearly a visible tail of rather small amplitude that is described by a much slower relaxation. A comparison with the lateral ACFs suggests that we encounter a classic example of weakly coupled degrees of freedom with a large difference in their time scales. The observed slow tails of the transverse ACFs repeat exactly the corresponding tails for the longitudinal relaxation. The semilog scale of the figure allows one to see the dominant relaxation time of the longitudinal ACFs although the ACFs are not perfectly straight and indicate some contribution from the faster modes in their initial decay. The fundamental longitudinal relaxation times can be estimated from the slopes of the linear part of the ACF rather reliably. The situation with the trasverse relaxation, however, is complicated by the fact that the initial relaxation contains also small-scale contributions from different modes whereas the long-term relaxation is dominated by coupling to lateral modes.

Part (b) of the Figure displays the normal ACFs for various values of  $N$  and two values of  $D$  in a log-log scale. It is clear that the major initial portion of the normal relaxation is  $N$ -independent although it depends strongly on the slit width. On the other hand, the long tails demonstrate a dependence on both  $N$  and  $D$  due to coupling, as one would expect for the longitudinal relaxation.

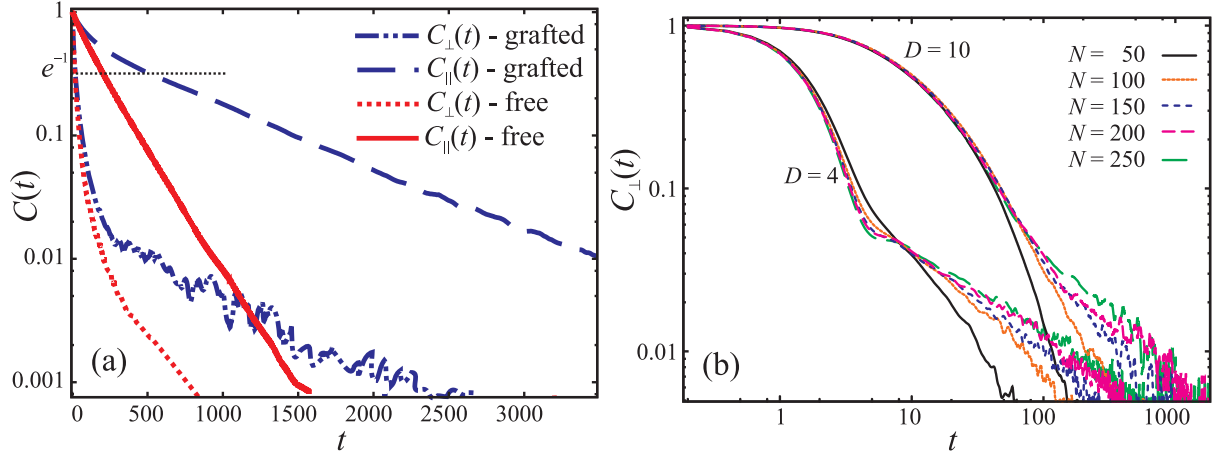


FIG. 8: (a) Comparison of the time autocorrelation functions (ACF) of the normal and parallel gyration radius components for grafted and free chains with  $N = 100$  in a slit with  $D = 10$ . The intersection of  $C_{\perp}(t)$  with the horizontal dotted line at  $e^{-1}$  has been used to determine the characteristic time of the fast chain relaxation perpendicular to the slit wall, shown in Fig. 8b. (b) Log-log plot of the ACF of the gyration radius normal component for two slit widths  $D = 4$  and  $D = 10$  and different chain lengths.

The scaling theory for the longitudinal relaxation time is rather straightforward and the main ideas were discussed before by Descas et al.<sup>47</sup>. The relaxation time scales as

$$\tau_{\parallel} \sim R^2 \zeta_{fr} \quad (31)$$

where  $\zeta_{fr}$  is the total chain friction coefficient. For a free-draining chain,  $\zeta_{fr} = N\zeta_0$  with  $\zeta_0$  being the friction per one monomer. It follows immediately that the relaxation time is proportional to a scaling parameter

$$\psi = N^{1+2\nu_2} (D + \delta)^{2(1-\nu_2/\nu)} \quad (32)$$

All the longitudinal relaxation times evaluated from the slopes of the gyration radius ACFs are plotted in Figure 9 against the scaling variable suggested by Eq. 32. The best fit for the relaxation times of non-grafted chains is

$$\tau_{\parallel} = 0.0053\psi. \quad (33)$$

It is natural to expect that the effect of grafting one of the chain ends is dynamically equivalent to doubling the chain length as far as longitudinal relaxation is concerned. In this picture, the grafted end is similar to the middle monomer of the doubled chain whose motion relative to the center of mass contributes very little to the lateral size relaxation. The data points for grafted chains are described very accurately by an equation based on this picture,

$$\tau_{\parallel} = 2^{5/2} 0.0053\psi. \quad (34)$$

The global translational diffusion coefficient of the confined chain was obtained from the mean square displacement of the center of mass as a function of time. All the curves are nearly ideal straight lines. According to the Einstein-Smoluchovsky equation for a 2-dimensional diffusion

$$\langle (r_{cm}(t) - r_{cm}(0))^2 \rangle = 4D_{diff} t = \frac{4}{N\zeta_0} t \quad (35)$$

The friction coefficient in our MD simulation comes from the thermostat coupling and is set to be equal to 0.5. Indeed, all the simulation results are in perfect numerical agreement with the theory. It is a commonly accepted convention to define characteristic diffusion time as a time required to reach the mean-square displacement equal to  $R^2$ . From this convention we obtain the following scaling fit for our model:

$$\tau_{diff} = 0.02\psi \quad (36)$$

Comparing Eqs. 33 and 36, we find that the ratio of the lateral diffusion time to the time of lateral relaxation amounts to a constant factor of about 3.8.

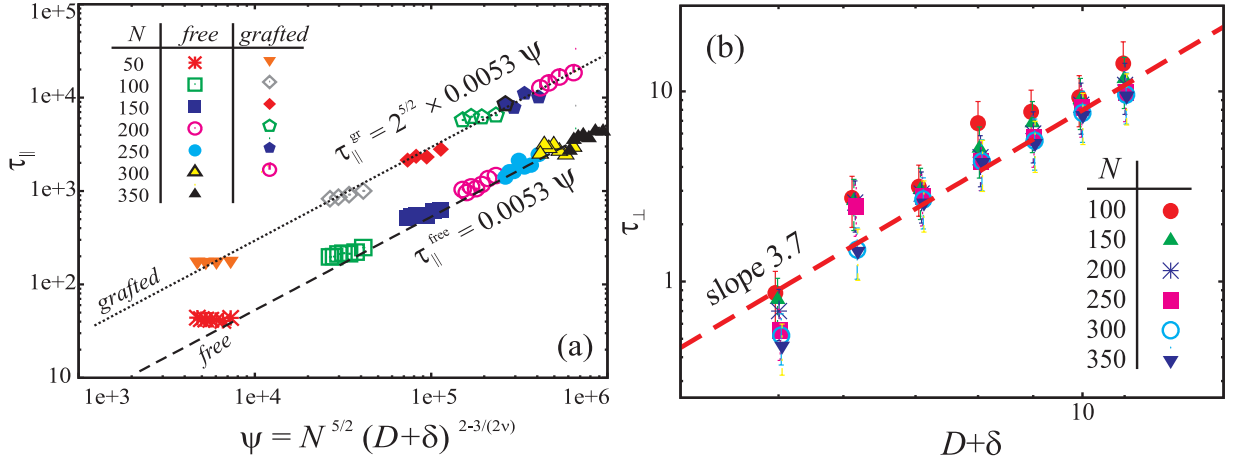


FIG. 9: (a) Mean relaxation times parallel to the slit wall for free and tethered chains with different length  $N$  in slits of width  $D$  against scaling variable  $\psi = N^{5/2}(D+\delta)^{2(1-\nu_2/\nu)}$ . Since a tethered chain relaxes effectively as a free chain of doubled length, the vertical offset of the straight lines in log-log coordinates is  $2^{5/2}$ , as expected - see text. (b) Characteristic time of the fast chain relaxation perpendicular to the slit wall against width  $D + \delta$  for chains of different length  $N$ . The straight line indicates the theoretically expected slope of  $2 + \nu^{-1}$ .

A scaling description for the normal relaxation is based on the idea that, as far as transversal motion is concerned, blobs relax independently. This would mean that both the normal end-to-end distance and the normal gyration radius are characterized by the same relaxation time of a single blob,

$$\tau_{\perp} \sim g^{1+2\nu} \sim D^{2+1/\nu} \quad (37)$$

As mentioned above, the shape of the transversal ACFs is far from being simple so that extracting a characteristic time requires caution. In order to evaluate the proper normal relaxation times we were subtracting the long-time tails due to coupling with longitudinal modes. After this subtraction, the shape of the ACFs allows for a better defined dominant transverse relaxation time.

The transverse relaxation times are presented in Figure 9b against the slit width  $D$  on a log-log scale for various chain lengths. The simulation data is consistent with the scaling prediction of Eq. 37 which gives  $\tau_{\perp} \propto D^{2+1/\nu}$ , being marked by a dashed best fit line in Fig. 9b:  $\tau_{\perp} = 0.002D^{2+1/\nu}$ . However, the accuracy is not very high as indicated by the error bars.

One can estimate numerically the typical time for normal relaxation, making use of Eq. 33, by noting that  $\tau_{\parallel}$  describes the relaxation of a single blob, provided one uses in  $\psi$  the number of monomers in a blob. This yields

$$\tau_{\perp} = 0.0053D^{2+1/\nu}. \quad (38)$$

which is proportional to the best fit line in Fig. 9b by a factor of  $\approx 2.7$ .

## V. SUMMARY AND DISCUSSION

In the present work we present a comprehensive study of the static and dynamic properties of flexible polymer chains confined in a narrow slit with impenetrable repulsive walls. A combination of extensive MD simulations and an analytic theory provides a consistent picture of polymer behavior parallel and normal to the slit walls.

- The confinement free energy (per blob) has been obtained rather precisely and shown to be equal very nearly to  $2k_B T$ .
- Exact, model-independent expressions with no adjustable parameters are derived for the normal components of the mean end-to-end distance and radius of gyration, and shown to be in excellent agreement with simulation data. Also in the case of grafted chains, closed analytic expressions for the end-to-end distance in normal direction were obtained for arbitrary positions of the grafting monomer.
- The observed size of the polymer parallel to slit walls is found to comply very well with scaling predictions in a broad interval of chain lengths and slit widths. The corresponding probability distribution functions are found analytically and confirmed by means of our computer experiments.

- The bond orientation profile across the slit was predicted analytically for Gaussian and real chains, and verified by simulation. The predicted average orientation for different slit widths has been found to agree very well with simulation data.
- The characteristic relaxation times of confined chains in directions parallel and normal to the slit walls have been obtained from evaluation of the respective autocorrelation functions. The effect of grafting on lateral relaxation time, which should be equivalent to doubling of the chain length, has been demonstrated.
- A novel feature is the observed coupling of normal and lateral modes with vastly different relaxation times.
- It is found that the mean diffusion times in lateral direction, albeit scaling similarly to the lateral relaxation time with chain length and slit width, are larger than the latter by a constant factor of about 3.8. The lateral relaxation time, evaluated for a single blob, is larger by the perpendicular relaxation time by a factor of 2.7.

It is interesting to note that the possibility to derive accurate analytic expressions for the static chain properties perpendicular to the slit planes is due to the screening of correlations between distant blobs in the direction of compression.

As mentioned before, the properties of the present system of a confined polymer are entirely determined by the underlying anisotropy in space. The situation is similar to that of adsorbed polymers on a plane where the thickness of the adsorbed layer is determined by the attraction to the surface and the chain conformations undergo deformation in perpendicular direction<sup>48</sup>. Therefore it is not surprising that the adsorbed chain dynamics is described by scaling theory in close analogy to the present treatment, as shown recently by Descas et al.<sup>47</sup>.

### Acknowledgments

We, L. I. K. and A. M. S., are grateful to the Deutsche Forschungsgemeinschaft (DFG) for financial support under Grant Nos. 436 RUS 113/863/0. A. M. S. received partial support under Grant NWO-RFBR 047.017.026. One of us (D. D.) appreciates support from the Max Planck Institute of Polymer Research via MPG fellowship, another (A. M.) received partial support from the DFG under project No. 436 BUL 113/130.

### Appendix

In order to evaluate an indirect orienting effect of the walls we take into account the fact that a bond experiences a torque due to the two tails attached to it. This torque is non-uniform as the partition functions of the tails depend on the position in the normal direction. The non-normalized weight for all configurations with the  $n$ -th monomer at position  $z$  and the  $n + 1$ -st monomer at position  $z' = z + a \cos \theta$  is given by the product of the partition functions of the two tails

$$W(z, \theta) = Q_n(z)Q_{N-n}(z + a \cos \theta) \quad (39)$$

Here we assume factorization which is exact for ideal chains. (This is also a plausible scaling ansatz for real chains in the strong confinement limit provided only normal directions are concerned). The partition function  $Q(z)$  is in fact the Green's function integrated over the positions of the other tail end. Up to a normalization factor it coincides with the probability distribution of free chain ends  $\rho_{\text{end}}(z)$ , and is therefore a function of the form  $Q(z) = \text{const} D^{-1} f(z/D)$ . For a confined ideal chain in the ground state approximation it is independent of  $n$  and is given by the ground state wavefunction of the Edwards' equation:

$$Q(z) = \text{const} \cdot D^{-1} \cos(\pi z/D) \quad (40)$$

Expanding  $Q(z + a \cos \theta)$  up to second order in  $\cos \theta$  we obtain

$$W(z, \theta) = Q^2(z) \left[ 1 + \frac{a}{D} \frac{f'}{f} \cos \theta + \frac{1}{2} \left( \frac{a}{D} \right)^2 \frac{f''}{f} \cos^2 \theta \right] \quad (41)$$

Calculating the average  $\langle \cos^2 \theta \rangle$  with the weight  $W$  up to the lowest non-trivial order in  $a/D$  gives the following result for the average Legendre polynomial

$$\langle P_2(z) \rangle = \frac{1}{15} \frac{f''(z/D)}{f(z/D)} \frac{a^2}{D^2} \quad (42)$$

In the general case this quantity is still a function of the  $z$  coordinate and has to be averaged over the slit width with the weight given by the full monomer density  $\rho(z)$ . However, for an ideal chain, the ratio  $f''/f = -\pi^2$  is constant at any position within the slit and won't be affected by averaging. This brings the final result

$$\langle P_2 \rangle_{\text{id}} = -\frac{\pi^2 a^2}{15D^2} \quad (43)$$

which means that the indirect orientation effect is dominant compared to the local wall effect  $\sim D^{-3}$

For a real chain, after averaging over the slit width we get a result very similar to Eq. 43. Only the numerical coefficient changes slightly but the  $D^{-2}$  dependence persists. Since the propagating effect of the wall is much stronger in this case, the indirect orientation by torque constitutes just a minor correction.

- <sup>1</sup> P. G. de Gennes, Phys. Lett. **38A**, 339(1972).
- <sup>2</sup> P. G. de Gennes, in *Scaling Concepts in Polymer Physics*, Cornell University Press, Ithaca, N. Y., 1979.
- <sup>3</sup> K. F. Freed, *Renormalization Group Theory of Macromolecules*, Wiley, New York, 1987.
- <sup>4</sup> J. des Cloizeaux and G. Jannink, *Polymers in Solutions: Their Modeling and Structure*, Clarendon, Oxford, 1990.
- <sup>5</sup> L. Schäfer, *Excluded Volume Effects in Polymer Solutions*, Springer, Berlin, 1999.
- <sup>6</sup> P. Flory, *Principles of Polymer Chemistry*, Cornell University Press, Ithaca, New York, 1953.
- <sup>7</sup> M. Daoud and P. G. de Gennes, J. Phys. (Paris) **38**, 85(1977).
- <sup>8</sup> F. Brochard and P. G. de Gennes, J. Phys. (Paris) **40**, L399 (1979).
- <sup>9</sup> I. Webman, J. L. Lebowitz and M. H. Kalos, J. Phys. (Paris) **41**, 579(1080).
- <sup>10</sup> K. Kremer and K. Binder, J. Chem. Phys. **81**, 6381(1984).
- <sup>11</sup> P. Cifra, T. Bleha and T. Romanov, Macromol. Chem. Rapid Commun. **9**, 355(1988).
- <sup>12</sup> T. Bleha, P. Cifra and F. E. Karasz, Polymer **31**, 1321(1990).
- <sup>13</sup> A. Milchev, W. Paul and K. Binder, Macromol. Theory Simul. **3**, 305 (1996).
- <sup>14</sup> A. P. Thompson and E. D. Glandt, Macromolecules, **29**, 4314(1994).
- <sup>15</sup> T. W. Burkhardt and I. Guin, Phys. Rev. E **59**, 5833 (1999).
- <sup>16</sup> Y. Wang and I. Teraoka, Macromolecules, **30**, 8473 (1997), *ibid.* **33**, 6901(2000).
- <sup>17</sup> A. Milchev and K. Binder, Eur. Phys. J. B **3**, 477 (1988), *ibid.* **13**, 607 (2000).
- <sup>18</sup> K. Hagita and H. Takano, J. Phys. Soc. Japan, **68**, 401(1999).
- <sup>19</sup> J. de Joannis, J. Jimenez, R. Rajagopalan, and I. Bitzani, Europhys. Lett. **51**, 41(2000).
- <sup>20</sup> P. Cifra, T. Bleha, Y. Wang, and I. Teraoka, J. Chem. Phys. **113**, 8313(2000).
- <sup>21</sup> P. Sotta, A. Lesne, and J. M. Victor, J. Chem. Phys. **112**, 1565 (2000).
- <sup>22</sup> M. Bishop and C. J. Saltiel, J. Chem. Phys. **66**, 606 (1991).
- <sup>23</sup> J. M. Victor and D. Lhuillier, J. Chem. Phys. **92**, 1362 (1990).
- <sup>24</sup> Y. J. Sheng and M. C. Wang, J. Chem. Phys. **114**, 4724(2001).
- <sup>25</sup> P. Cifra and I. Teraoka, Polymer **43**, 2409 (2002).
- <sup>26</sup> P. Cifra, T. Bleha, Macromolecules, **34**, 605 (2001).
- <sup>27</sup> H. P. Hsu and P. Grassberger, J. Chem. Phys. **120**, 2034 (2004).
- <sup>28</sup> I. Teraoka, P. Cifra, and Y. Wang, Colloids and Surf. **206**, 299 (2002).
- <sup>29</sup> H. P. Hsu and P. Grassberger, Eur. Phys. J. E **36**, 209 (2003).
- <sup>30</sup> I. Teraoka and P. Cifra, Polymer **43**, 3025 (2002).
- <sup>31</sup> I. Teraoka and Y. Wang, Polymer **45**, 3835 (2004).
- <sup>32</sup> E. Eisenriegler, *Polymers near Surfaces*, World Scientific, Singapore, 1993.
- <sup>33</sup> P. G. de Gennes, Macromolecules, **14**, 1637 (1981).
- <sup>34</sup> E. Eisenriegler, K. Kremer, and K. Binder, J. Chem. Phys. **77**, 6296 (1982).
- <sup>35</sup> P. G. de Gennes and P. Pincus, J. Phys. Lett. **44**, L241 (1983).
- <sup>36</sup> P. Grassberger, Phys. Rev. E **56**, 3682 (1997).
- <sup>37</sup> G. S. Grest and K. Kremer, Phys. Rev. A **33**, 3628 (1986).
- <sup>38</sup> H. Clausen-Schaumann, M. Seirz, R. Krautbauer, and H. E. gaub, Curr. Opin. Chem. Biol. **4**, 524 (2001).
- <sup>39</sup> M. C. Williams and I. Rouzund, Curr. Opin. Chem. Biol. **12**, 330 (2002).
- <sup>40</sup> K. Binder (ed. *Monte Carlo and Molecular Dynamics Simulations in Polymer Science*, Oxford Univ. Press, N.-Y., 1995).
- <sup>41</sup> M. Kotelyanskii and D. N. Theodoru, *Computer Simulation Methods for Polymers*, M. Dekker, N.-Y., 2004.
- <sup>42</sup> M. P. Allen and D. J. Tildesley, *Computer Simulations of Liquids*, Clarendon Press, Oxford, 1987.
- <sup>43</sup> M. Fisher, J. Chem. Phys. **44**, 616 (1966).
- <sup>44</sup> S. Caracciolo, M. S. Causo, and A. Pellissetto, J. Phys. A **32**, 1215 (1998).
- <sup>45</sup> J. P. Wittmer et al. Phys. Rev. Lett. **93**, 147801 (2004).
- <sup>46</sup> A. Milchev and K. Binder, J. Phys. II France, **6**, 21 (1996).
- <sup>47</sup> R. Descas, J.-U. Sommer, and A. Blumen, J. Chem. Phys. **122**, 134903 (2005).
- <sup>48</sup> A. Milchev and K. Binder, Macromolecules, **29**, 343 (1996).